Production of Ultracold Neutrons

Troy Dawson

May 5, 2009

Abstract

The recently proposed CSUN source at TRIUMF aims to have the highest UCN density, and will be used to complete fundamental physics experiments. Neutron production from a spallation-driven superfluid-helium UCN source was studied. A Monte Carlo simulation code was used to create a model of this source. The model was used to determine the impact of γ-shield thickness on the cold neutron flux and heat deposition within the source. The results indicate constant cold neutron flux and decreasing heat deposition as the shield thickness was increased. This relationship could be important because of the higher beam power used in the TRIUMF source relative to the prototype source in Japan. The results compare favourably with previous results from the Japanese group.

Contents

1 Introduction

Neutrons were discovered in 1932 by James Chadwick (Nobel Prize - 1935). They are generally bound within atomic nuclei with protons. Free neutrons can be liberated from the nuclei of atoms. Free neutrons are used in physics experiments worldwide. Neutrons are able to deeply probe materials, due largely to their lack of electric charge. There is also considerable interest in studying the fundamental interactions of the free neutron, for example its lifetime and electric dipole moment. Table 1 contains various fundamental properties of free neutrons.

Mass	$939.56563 \pm .00008\ [\frac{MeV}{c^2}]$
Mean Lifetime	$885.7 \pm 0.8\ [seconds]$
Magnetic Moment	$(-1.9130427 \pm .0000005)\ \mu_N$
Electric Dipole Moment	$< 2.8 \times 10^{-26}\ [e \cdot cm]$ [3]
Charge	$(-0.4 \pm 1.1) \times 10^{-21}\ e$
Spin	$\frac{1}{2}$

Table 1: Collection of fundamental neutron properties [2]. Neutron lifetime and electric dipole moment values are both obtained from experiments involving ultracold neutrons, discussed is section 1.2. Neutron mass and magnetic moments are of interest for neutron interactions, discussed in section 2.3.

After successful experiments in 1946 and 1947 Fermi experimentally demonstrated total reflection of a neutron from a material surface. This led to the successful implementation of neutron guide tubes which are used to allow neutrons to travel in a fixed direction, assuming that the neutron energy was low enough. In 1959, Zeldovich proposed total storage of a neutron in a material bottle, which would be achieved if a neutron had a energy low enough to be completely confined by what is now known as the Fermi potential of a material [1]. Neutrons that are capable of storage in a bottle, which requires elastic collisions from the surface of the material walls of the bottle, are known as ultracold neutrons.

1.1 Ultracold Neutrons

Free neutrons are classified according to their kinetic energy. A definition of different neutron energies can be found in table 2. It is important to distinguish between different neutron energies

because neutrons at higher energies penetrate deeply into materials. Cold and ultracold neutrons do not. Ultracold neutrons (UCN) are extremely useful for certain experiments probing fundamental particle interactions because of the ability to store them for long periods of time. Section 2 details neutron interactions as a function of kinetic energy in greater detail.

Level	Typical Kinetic Energy (eV)
Fast	$\geq 10^5$
Thermal	≈ 0.025
Cold	$\geq 10^{-6}$
Ultracold	$\leq 300 \times 10^{-9}$

Table 2: Various types of neutrons. Fast neutrons are produced when the neutrons are liberated from atomic nuclei, see section 3.1. Thermal neutrons are neutrons at thermal equilibrium with a moderator at 300 K, discussed in section 2.2.1. Cold neutrons are produced from a cold moderator, $T \leq 20$ K. Ultracold neutrons can produced through downscattering in superfluid helium, discussed in section 2.2.2.

1.2 Experiments of interest involving UCN

UCN sources are characterized by UCN density ρ_{UCN} available to experiments. The higher the density of ultracold neutrons available for experiment, the higher the level of accuracy achievable, since statistical errors can be reduced. Additionally, systematic uncertainties can often be reduced as well because new experimental techniques become available that were not at lower ρ_{UCN}. Three modern-day experiments using UCN to probe fundamental interactions are the following:

- A search for a non-zero electric dipole moment of a neutron.
- A precise measurement of the lifetime of a free neutron.
- Characterization of UCN quantum states present in the earth's gravitational field.

Each experiment has its own fundamental physics interest, and each experiment will be briefly described here.

1.2.1 Neutron Electric Dipole Moment (n-EDM)

Due to time-reversal symmetry, electric dipole moments are forbidden for fundamental particles. However, a small amount of CP violation is present in the standard model that leads to extremely small EDM's. The product of charge conjugation (C) and parity (P) inversions is CP symmetry, which is invariant for strong and electroweak interactions. CP violation is a violation of CP symmetry present during certain types of weak decays. The expected zero EDM is related to time-reversal (T) via the CPT theorem. CPT symmetry is a fundamental symmetry that physical laws are invariant under simultaneous time, parity and charge inversion.

The predicted EDM for a neutron in the standard model is on the order of 10^{-31} e·cm. Current experimental data has confined the n-EDM to $d_n < 2.9 \times 10^{-26}$ e·cm. Certain models which allow a greater level of CP violation, such as supersymmetry, predict $d_n \approx 10^{-28}$ e·cm. UCN densities exceeding 1000 UCN/cc are required constrain d_n further. New UCN sources are needed with the hope to constrain d_n at the 10^{-28} e·cm level. Next generation experiments are being prepared aiming for this level of precision.

1.2.2 Neutron Lifetime

Neutrons undergo beta decay via the weak interaction (discussed in section 2.3.3). A precision measurement of the neutron lifetime is an important parameter for Big-Bang Nucleosynthesis calculations, a theory describing the production of elements heavier than ^{1}H in the minutes following the big bang. The neutron lifetime is important in these calculations due to the weak interactions and conversions between neutrons and protons. Neutron lifetime can also be used to measure the Cabibbo−Kobayashi−Maskawa (CKM) matrix parameter V_{ud}. The CKM matrix is used to explain quark mixing during weak interactions. The CKM matrix is unitary, assuming there is no unknown physics missing, however, the current errors associated with the matrix elements are too large to accurately determine if it is in fact unitary. To make the extraction of V_{ud}, it is also necessary to measure angular correlation in neutron decay, but the uncertainty on neutron lifetime currently dominates the extraction.

Neutron lifetime measurements have been done by storing UCN in a material bottle, waiting a time to allow some neutrons to decay, and then emptying the bottle and counting the number of neutrons that come out. Preforming this experiment for different storage times allows for an extraction of n-lifetime. The main source of error in this experiment arises due to wall losses.

This error can be greatly reduced if the neutrons are confined in a magnetic trap instead of a material trap. A magnetic trap capable of significantly reduced systematic uncertainties has been designed and is being constructed at Los Alamos National Lab. The experiment is awaiting a new UCN source with a large enough density ($\rho_{\mathrm{UCN}} \approx 100$ UCN/cc) to produce a statistically accurate measurement of neutron lifetime.

Currently, the world average for the lifetime of a neutron is ($885.7 \pm 0.8s$). But a new experiment using a very similar experimental technique disagrees with this value by 6.5 standard deviations [6]. It is therefore important to conduct a new high-precision measurement using a magnetic trap at a new, high-density UCN source.

1.2.3 Quantized Neutron Energy Levels in Earth's Gravity Field

Recently, neutrons have been discovered to be confined to quantum energy levels in Earth's gravitational field. UCN are confined above by a UCN mirror in 1D by gravity. Classically, the neutrons would be expected to bounce up and down off the mirror. However, experimentally the neutrons are confined to wavefunctions of a particle in a 1D potential well [5]. New detectors capable of detecting neutrons on the micron level are being developed for successful implementation of such an experiment capable to probe short range gravitational interactions. A higher precision experiment would require high UCN densities for improved spectroscopy of the energy levels.

1.3 Worldwide UCN sources

Ultracold neutron sources are in high demand, due to their ability to probe fundamental particle interactions at a new level of accuracy. Different sources built using different technologies are currently being built world wide. Specific information presented in this paper reflect the design and development of the TRIUMF (TRI University Meson Facility) UCN source. Table 3 is a

summary of the technologies and expected UCN density output available for the experiment. The Los Alamos National Lab (LANL) source is currently in operation, along with the Paul-Scherrer-Institut source (PSI). All other sources are either proposed new sources or upgrades to existing sources (ILL Grenoble). The Canadian project at TRIUMF would exceed the capabilities of all projects worldwide.

Location	Technology	critical energy E_c (neV)	storage time τ_s (s)	density in experiment ρ_{UCN} (UCN/cm^3)
TRIUMF	spallation He-II	210	150	$1 - 5 \times 10^4$
ILL Grenoble	CN beam He-II	250	150	1000
SNS ORNL	CN beam He-II	134	500	150
Munich	reactor SD_2	250		10^4
NCSU	reactor SD_2	335		1000
PSI	spallation SD_2	250	6	1000
LANL	spallation SD_2	250	1.6	145

Table 3: Current and Future UCN sources worldwide. The range indicated for the TRIUMF source is due to the use of different cold moderators, discussed in section 3.[4]

2 Theory of Neutron Interactions

2.1 Neutron Flux

The neutron flux density, ϕ_n, is the number of neutrons per unit time passing through an infinitesimal volume divided by the area of that volume. Given an average number of neutrons, $< N >$, passing through a cross-sectional area, A, in time, t, then the flux can be defined as:

$$\phi_n = \frac{< N >}{At}$$

This gives the neutron flux units of neutrons/area/time [2].

2.2 Interactions of Higher Energy Neutrons with Matter

2.2.1 Moderation and Thermalization

Fast neutrons' energies can be reduced by a process known as moderation. Moderation involves scattering neutrons from a material, in which most of the neutron's energy is transferred to the target nuclei.

The ideal moderator will have a mass similar to that of a neutron, because this results in the largest average momentum transfer. In terms of mass, hydrogen (^{1}H) is the best, as the mass of a neutron is nearly the mass of a proton. Light water is the most widely used nuclear moderator in light water reactors, due to cheap cost, and high proton density (liquid at room temperature). However, light water can not be used for a UCN source, as the neutron capture cross section for hydrogen is too high to achieve desirable densities of UCN. Hydrogen has a neutron capture cross section of $\sigma_h = (0.329 \pm 0.004)$ barn [9]. Deuterium (^{2}H or D) has a neutron capture cross section of $\sigma_d = (0.000508 \pm 0.015)$ barn [10], which is 0.15% of the value for ^{1}H. These values given are for thermal neutrons. This difference results in neutron fluxes much greater from a heavy water moderator (D_2O) than what would be expected from using a light water moderator.

The thermal neutron absorption mean free path, $\bar{l}$, is given by

$$\bar{l} = \left(\frac{\rho \sigma N_A}{A}\right)^{-1}$$

where ρ is the mass density of the material, N_A is Avogadro's number, and A is the atomic mass of the moderator [11].

Since $\bar{l} \propto \frac{1}{\sigma}$, D_2O will have a longer diffusion length than H_2O. The values listed in table 4 confirm this result.

Suppose we consider the case where the target nuclei are of equal mass as the neutron, such would be the case for a proton moderator. From kinematics, on average 50% of the neutrons's energy will be transferred to the moderator nucleus per collision.

Material	Density	Slowing Time	Slowing down length	Diffusion length
	$(\frac{g}{cm^3})$	(μ s)	(cm)	(cm)
H_2O	1.0	10	5.7	2.9
D_2O	1.1	67	11	100
Beryllium	1.8	46	9.9	23.6
Graphite	1.6	150	19	50.2

Table 4: Neutron transport properties for some Neutron Moderators. Slowing time is the time required to slow a 2 MeV fast neutron to a thermal neutron. Slowing down length is the RMS distance a fast neutron will travel before being thermalized. Diffusion length is the average distance a thermal neutron will travel before being absorbed by the material [19].

The average energy after N collisions, assuming an initial energy of E_0 will be:

$$\langle E \rangle_N = \left(\frac{1}{2}\right)^N E_0$$

If a fast neutron enters the thermal moderator, with $E_0 = 5$ MeV, it will take, on average, 28 collisions to thermalize the fast neutron until $\langle E \rangle_N = 0.025$ eV [11].

Considering heavier nuclei, we may apply Fermi theory [12]:

$$\langle E \rangle_N = E_0 e^{-\zeta N}$$

with

$$\zeta = \left[\ln \frac{E}{E'}\right]_{av}$$

where ζ is the lethargy or recoil factor of the moderating nuclei.

Conservation of momentum and energy defines the ratio of energy transferred between the initial (E) and final (E') state after one collision as

$$\frac{E'}{E} = \frac{A^2 + 1 + 2A\cos\theta}{(A+1)^2} = e^{\zeta}$$

where A is the mass of the moderating atom.

Averaging over angular yields:

$$\zeta = 1 + \frac{(A-1)^2}{2A} \ln\left(\frac{A-1}{A+1}\right)$$

Thus, after N collisions,

$$\ln(E') = \ln(E) - N\zeta$$

which follows from the definition of lethargy.

Lethargy values for some nuclei can be found in Table 5 along with N for thermalization.

Nucleus	Lethargy (ζ)	N for thermalization
H	1.00	18
D	0.725	25
^{4}He	0.425	43
^{12}C	0.158	110
^{16}O	0.120	150

Table 5: Lethargy values for various neutron moderators and number of collisions for thermalization given a starting energy of 2 MeV [12]. Light nuclei are better moderators, shown by the high lethargy value and low N.

An ideal moderator will have a high lethargy along with a diffusion length that is larger than the slowing down length of the moderator. A high lethargy value ensures efficient collisions, reducing the number of collisions needed for thermalization, and a diffusion length being longer than the slowing down length ensures that the neutron is moderated before it is absorbed by the moderator.

With fast incident neutrons, it is a good approximation to treat the moderator as a collection of static nuclei, due to the large energy difference. However, neutrons in thermal equilibrium can not be treated in this manner, as their kinetic energies are similar to the kinetic energy of the molecules in the moderators. Thus, neutrons in thermal equilibrium with their surroundings exhibit properties similar to that of an ideal gas. On average, the neutrons will be at the same temperature, T, as their environment. The actual speed on the individual neutrons will be given by the Maxwell-Boltzmann distribution, defined as:

$$f(v)dv = 4\pi n \left(\frac{m_n}{2\pi k_b T}\right)^{3/2} \cdot v^2 \cdot e^{-\frac{m_n v^2}{2k_b T}} dv$$

where $f(v)dv$ gives the fraction of neutrons with speeds between v and $v+dv$, n is the total number of neutrons per unit volume and m_n is the neutron mass. In terms of energy;

$$f(E)dE = \frac{2\pi n}{(\pi kT)^{3/2}} \cdot E^{\frac{1}{2}} \cdot e^{-\frac{E}{k_b T}} dE$$

where $f(E)dE$ gives the fraction of neutrons with kinetic energies between E and $E+dE$. Plotting this for all energies results in a curve showing a distribution of neutron energies at a specific temperature T.

This curve is shown schematically in Fig. 1. For 300 K the average energy is 0.0259 eV. For 20 K the average energy is 0.00172 eV.

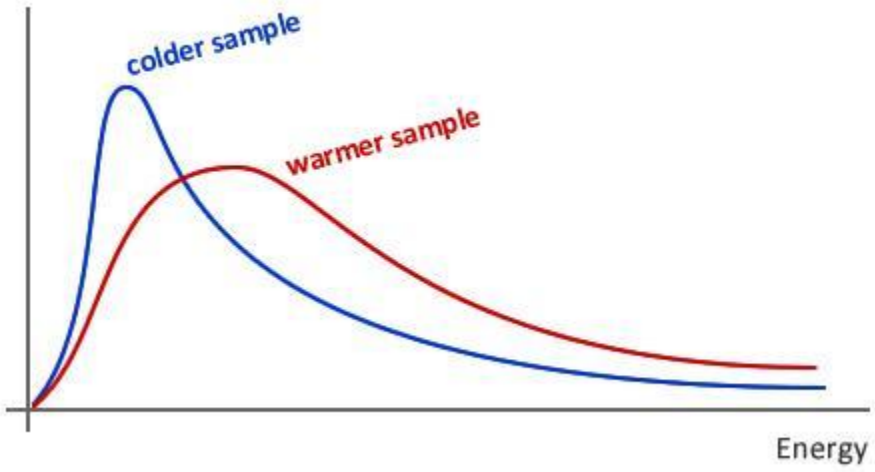

Figure 1: Two Maxwell-Boltzmann Distributions, showing two different temperatures. The vertical axis is $f(E)$. [17]

Some properties of thermalization relating to UCN are the following:

- No neutrons at velocity $v = 0$, as expected from the third law of thermodynamics
- Even at high temperature, there is (an extremely small) potential for individual neutrons to be UCN

However, this method of creating UCN is not efficient.

2.2.2 Downscattering

We now describe a method of efficiently creating UCN directly from a source of cold neutrons. This process is known as downscattering. Downscattering is the process by which cold neutrons lose energy to a solid or liquid via phonon production. Superfluid helium is an excellent downscattering medium because it does not absorb neutrons and has a desirable scattering length. It also has a single phonon excitation in the appropriate cold neutron energy range, as will be discussed. The production rate of UCN by downscattering is given by [8]:

$$P_{UCN} = \int\int \sigma(E_{in} \rightarrow E_{UCN})\, \phi(E_{in})\, N\, dE_{in}\, dE_{UCN}$$

Here $\sigma(E_{in} \rightarrow E_{UCN})$ is the downscattering cross-section, $\phi(E_{in})$ is the incident cold neutron flux and N is the nuclear number density.

The downscattering cross-section is related to the neutron scattering length a, the energy difference between initial and final energies $\hbar\omega = E - E'$, the momentum transfer $q = k - k'$, and the dynamic scattering function $S(q, \hbar\omega)$ such that:

$$\sigma = 4\pi a^2 \frac{k'}{k} S(q, \hbar\omega)$$

For ^{4}He, the scattering length is 3.26 fm [13] and the dynamic scattering function can evaluated for different values on the dispersion curve, as detailed in [14].

In the cold neutron energy range, the energy-momentum dispersion curves cross for Helium-II phonons and neutrons. At the intersection point, phonons behave like neutrons, allowing energy to be efficiently transfered from the neutrons into the helium-II. For superfluid helium $S(q, \hbar\omega)$ is strongly peaked at $q = 8.9$Å which is equal to the kinetic energy of cold neutrons at 12 K. When the cold neutrons strike the superfluid, energy and momentum is transferred to the helium, reducing the cold neutron's energies to ultracold levels. Multiphonon processes can give non-zero $S(q, \hbar\omega)$ at smaller wavelengths.

The reverse process, upscattering, can be suppressed by keeping the helium cooled to $T \leq 1$ K [7].

In general the UCN density ρ_{UCN}, of a source may be calculated from the production rate as:

$$\rho_{UCN} = P_{UCN} \times \tau_s$$

where τ_s is the storage lifetime. The value for τ_s is governed by surface quality and geometry of the bottle. A typical value for a 100 cm^3 bottle is 100 s. P_{UCN} is governed by solid state physics of the UCN production material, described above for helium.

2.3 Ultracold Neutron Interactions

Ultracold neutrons interact with matter via the strong, weak, magnetic and gravitational fields. Some aspects regarding each of these interactions will now be discussed.

2.3.1 Interactions with magnetic fields

External magnetic fields, $\vec{B}$, interacting with the magnetic moment of a neutron, $\vec{\mu}_n$, produces a potential energy,

$$V_m = -\vec{\mu}_n \cdot \vec{B}.$$

Ultracold neutrons have a magnetic moment of $(-1.9130427 \pm .0000005)\mu_N$, with μ_N being the nuclear magneton, equal to

$$\mu_N = \frac{e\hbar}{2m_p} = 31.52\ neV/T$$

resulting in a magnetic moment of a neutron to be 60 neV/T in magnitude. The magnetic field will apply a force to the neutron equal to:

$$F_m = -\vec{\nabla} V_m$$

The inhomogeneous field seen by the neutron as it moves through the magnetic field must be less then the Larmor frequency of the magnetic moment in the field, thus requiring ultracold neutrons and a relatively smooth field profile. If the neutrons are moving too fast (i.e. not UCN) through the magnetic field, the Larmor frequency seen by the neutrons will be too large, and can lead to a

spin flip of the neutron. The UCN are then said to satisfy the adiabatic condition [1]

$$\frac{v \cdot \frac{dB}{dz}}{B} << \omega_{Larmor}$$

Assuming this condition is satisfied, a magnetic bottle will occur for a minimum in $\left|\vec{B}\right|$ for a one neutron spin state. A magnetic bottle depth of ≈ 6 T would trap UCN because $\Delta V = \mu_N \Delta B =$ 360 neV and the UCN have energies of < 300 neV.

2.3.2 Interactions with gravity

Gravitational potential energy is given by:

$$V_g = m_n g h$$

where for neutrons $m_n g = 102 \times 10^{-9} eV \cdot m^{-1}$. An ultracold neutron with a kinetic energy equal to 300 neV will therefore rise three metres before being overcome by gravity and returning to earth. Gravity can be used, by placing a detector or guide beam for UCN at specific heights, as a energy selector, since different heights allow for significant amounts of energy to be transferred to or taken away from the ultracold neutron [1]. Also, new experiments involving ultracold neutrons have been developed to probe the quantum nature of short range gravitational interactions [5].

2.3.3 Interactions with the weak nuclear force

Free neutrons are not stable. The main effect of the weak force on an ultracold neutron, or free neutrons in general is that it causes it to decay. The main decay path is:

$$n \rightarrow p + e^{-} + \bar{\nu}_e$$

This is the decay that is present in the lifetime of a neutron experiment, as discussed in section 1.2.2. When a neutron is in a bound state, for example in the nucleus of an atom, decay is not energetically favorable. The decay reaction for free neutrons produces only 782 keV of energy, much

less then a typical nuclear binding energy, which is on the order of a few MeV [1]. The neutron will not decay as the decay reaction does not produce enough energy to break the nucleus apart.

2.3.4 Interactions with the strong nuclear force

The strong force is what binds neutrons and protons together within a nucleus. The neutrons and protons are confined within the nucleus by a potential well present due to the strong force. The electrostatic effects between the protons in the nucleus are much smaller than the well depth, and thus the nucleus is bound together. The well can be approximated as a spherical square well. The will is typically $V_0 = 40$ meV deep and a few $r_0 = 2$ fm in radius.

Free incident neutrons upon a target nucleus will scatter off this potential, with either a positive or negative scattering length dependent in the details of the potential.

The effective potential, or Fermi pseudopotential, is what a neutron incident on a collection of nuclei in a solid would experience. In scattering theory, the Fermi pseudopotential can be modeled as a collection of delta-function potentials, each representing an atomic nucleus, as follows:

$$V_{eff}(\vec{x}) = \gamma\delta(\vec{x})$$

The differential cross section for scattering is

$$\frac{d\sigma}{d\Omega} = |f(\theta,\phi)|^2$$

and may be calculated using the Born approximation for low energy neutron scattering, (valid for weak scattering) as:

$$f(\theta,\phi) = -\left(\frac{m_n}{2\pi\hbar^2}\right)\int d\vec{r}\cdot e^{i\vec{\kappa}\cdot\vec{r}}V(\vec{r}) = -\frac{m_n}{2\pi\hbar^2}\gamma$$

where $\vec{\kappa} = \vec{k} - \vec{k'}$ is the momentum transfer.

For low-energy scattering off a well, $f(\theta,\phi) = -a$, where a is called the scattering length, and only the $l = 0$ partial wave is assumed to contribute. Comparing these results, we see that we can

replace the spherical well potential with a δ-function potential with $\gamma = \frac{2\pi\hbar^2 a}{m_n}$. Integrating over the many δ-functions in a material gives:

$$V_{eff} = \gamma n = \frac{2\pi\hbar^2 a n}{m_n}$$

and n is the nuclear number density. We see therefore that as long as a material has a positive a, it will have a repulsive effective potential.

If a material has a positive Fermi potential, and the incident neutron energy is less than this potential, the neutron will be completely reflected by this surface. Ultracold neutrons are defined to be neutrons which will undergo complete elastic scattering from a material wall. A list of Fermi pseudopotentials can be found in table 6.

Material	Density ($\frac{g}{cm^3}$)	Potential (neV)
Be	1.83	252
BeO	3.0	261
H_2O	1.0	-14.7
Al	2.7	54
C	2.0	180
Ti	4.54	-48
Fe	7.9	210
Ni	8.8	252
^{58}Ni	8.8	335
Cu	8.5	168
^{65}Cu	8.5	244
Pb	11.3	83

Table 6: Fermi psuedopotential for various materials[1]

UCN guides usually use Ni, ^{58}Ni, Cu, ^{65}Cu, Fe or C as their surface for this reason. It is the height of this potential that usually defines the energies available in any given experiment.

3 UCN Production and Sources

The newly proposed UCN source at TRIUMF by the Canadian Spallation Ultracold Neutron group (CSUN) is displayed schematically in Fig. 2. Here a proton beam strikes the spallation target

producing a random distribution of fast neutrons. The graphite shielding will reflect and focus stray neutrons towards the centre of the He-II bottle. The fast neutrons will be moderated in both the 300 K D_2O and 20 K D_2O, producing cold neutrons. These cold neutrons then enter the superfluid helium and become UCN by downscattering. The UCN then diffuse down the UCN guide tube and out to the experimental area. Also shown on the diagram is the radioactive shielding of the source along with the heat exchange system for maintaining the helium at 0.8 K.

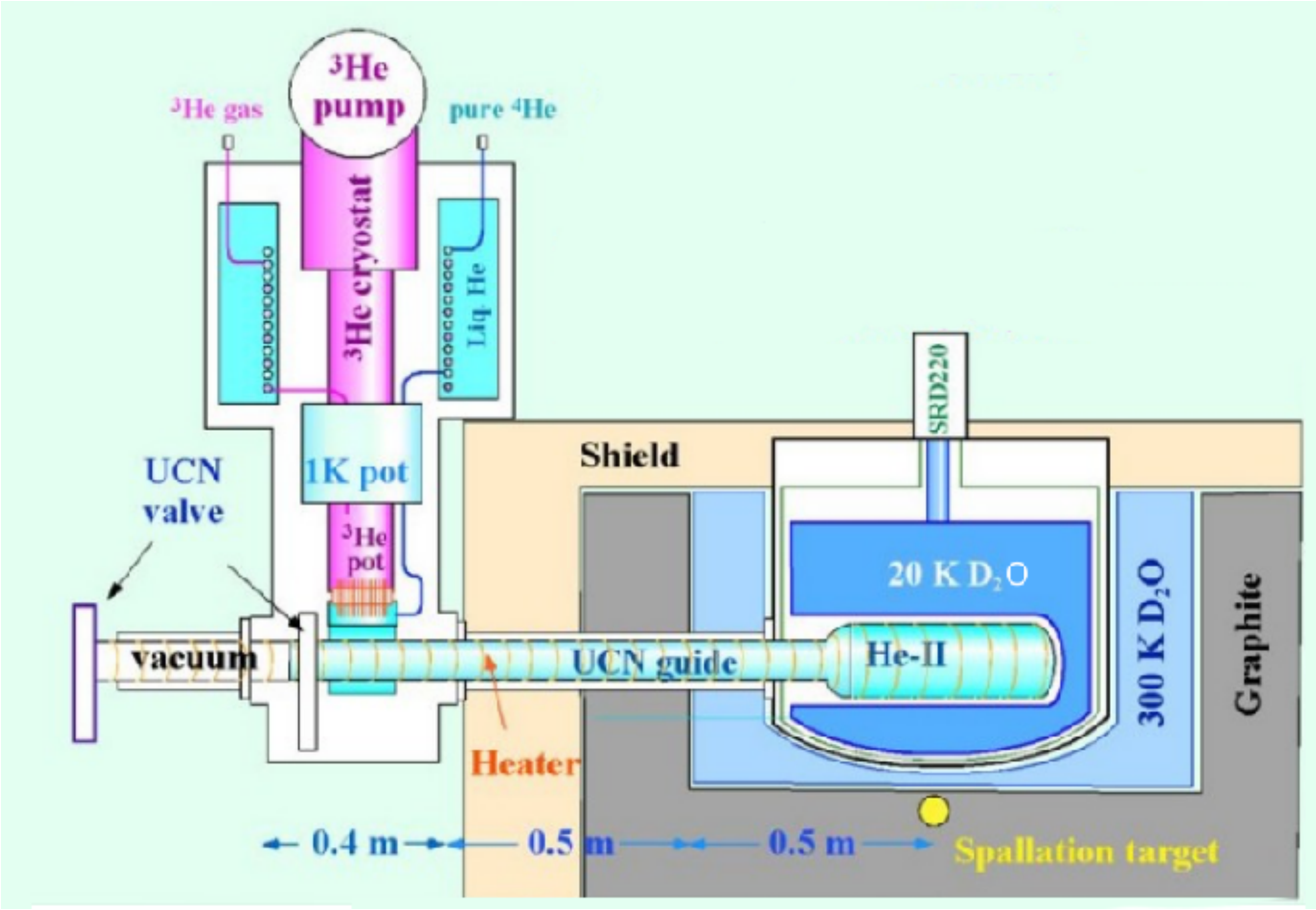

Figure 2: Schematic diagram of the proposed TRIUMF UCN source.

Some details regarding each process used in the creation of UCN will now be discussed.

3.1 Spallation

TRIUMF's 500 MeV proton beam will be used to produce fast neutrons, through a process known as spallation. Spallation is the process by which a heavy nucleus is struck by a high energy particle

producing several lighter nuclei and particles. These produced particles include protons, neutrons or α-rays. These particles can then strike nearby target nuclei repeating the process, creating a internuclear cascade. These particles can also be ejected from the target, producing the desired free neutrons.

Spallation yields have been calculated for various different proton energies, as illustrated in Fig. 3, with values given in fast neutrons produced per incident proton. The new CSUN source will use tungsten as the target. Tungsten has similar nuclear properties to lead and bismuth, allowing previous experimental data to be used, but more desirable thermal properties, allowing for simplified target design. Table 7 lists some common atomic data for these three elements. TRIUMF's 500 MeV proton beam can be expected to produce between 6.7 and 8.5 fast neutrons per incident proton [15][16].

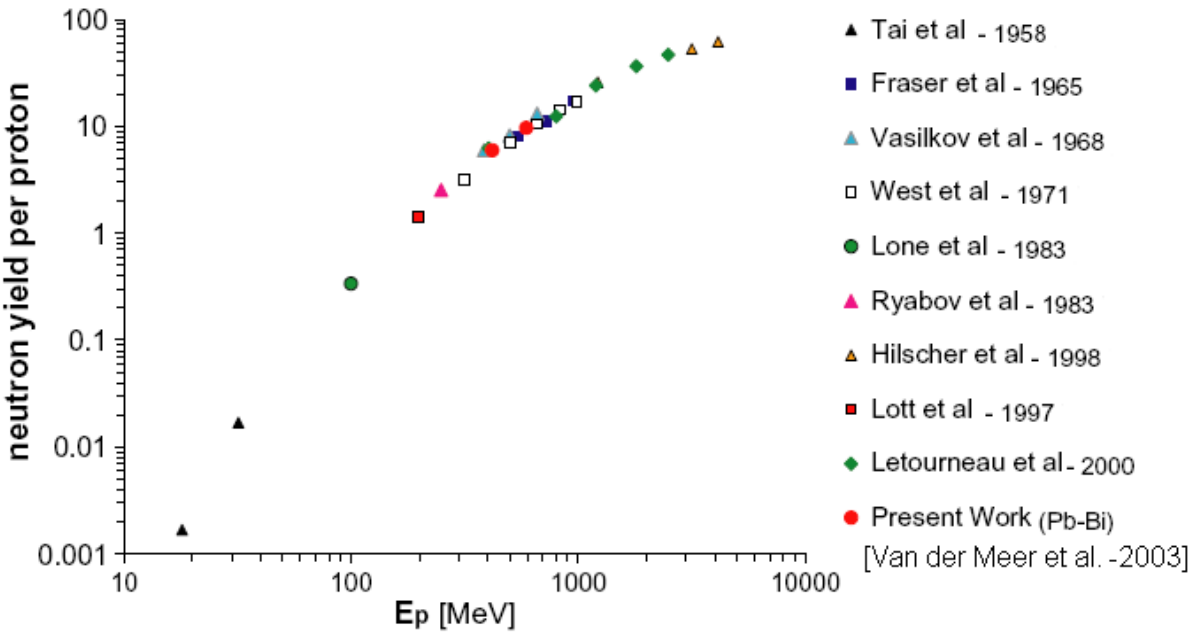

Figure 3: Spallation yields for Pb and Pb/Bi targets[15]

Fast neutrons are the primary radiation concern, along with the gamma's produced from the tungsten being used as, essentially, a beam dump. It is estimated that 150 m^3 of steel and 450 m^3 of concrete will be required to shield the spallation target to accepted dosage rates outside the shielding, as discussed in [4].

Element	Atomic Number Z	Neutron Number N	Atomic Mass $(\frac{g}{mol})$	Density $(\frac{g}{cm^3}, 300K)$	Melting Point (K)
Pb	82	124,125,126	207.2	11.34	600.6
Bi	83	126	208.98	9.78	544.7
W	74	108,109,110,112	183.84	19.25	3695

Table 7: Selected properties for potential spallation targets. The different number of neutrons present in each nucleus is due to naturally occurring isotopes. The listed atomic mass is an average based on isotopic abundance.

3.2 Moderation

As discussed in section 2.2.1, neutrons thermalize with their surrounding environment by a process known as moderation. The source design for TRIUMF includes two moderators, a room temperature (300K) heavy water moderator used to create thermal neutrons, along with another moderator to convert thermal neutrons to cold neutrons. From table 4, for heavy water, the source requires 11cm of moderator to thermalize a 2 MeV incident fast neutron, representing 25 collisions between ^{2}H and neutrons. Initially, the cold moderator will be 20 K D_2O, with an expected upgrade to 20 K liquid D_2. To cool thermal neutrons down to cold temperatures, an estimated 4 collisions is required. The upgrade to D_2 is expected to increase UCN density by a factor of five [4]. The graphite shown in Fig. 2 is used to reflect neutrons back into the 300K moderator, increasing the neutron flux.

3.3 Downscattering

Cold neutrons generated through moderation will enter a volume of superfluid helium, allowing for UCN to be produced through downscattering. The temperature of a cold neutron moderator results in an effective neutron temperature that is greater then the actual moderator temperature. For heavy water at 20 K, the effective neutron temperature is 80 K, which results in an average neutron wavelength of 3.46 Å [4]. For optimal UCN production in superfluid helium, neutron wavelengths of 8.9 Å are desired, as discussed in section 2.2.2. This results in an effective neutron temperature of $\approx$ 12 K. Liquid D_2 at 4 K has a greater number of neutrons effectively at this temperature, resulting in the increased UCN density. The lower effective neutron energy results from the lower neutron capture cross section, along with the lower moderator temperature [18],

which are present in the D_2.

The reverse process, upscattering, must be suppressed, requiring a constant temperature of $T \approx 0.8$ K. This can be maintained through heat exchangers with cryogenic ^{3}He and the superfluid helium within the source. By circulating the ^{3}He through the superfluid ^{4}He, heat is transfered to the ^{3}He via vapourization, which can then be removed from the ^{3}He via pumping. At 0.8 K, the saturated vapour pressure of ^{3}He is 3 Torr. A pumping speed of 1×10^4 m^3/h for ^{3}He at 3 Torr removes 17 W of heat. Preliminary calculations have showed that heating in the superfluid at TRIUMF will be manageable [4].

3.4 Guide to Experimental Area

Ultracold neutrons are guided to the experimental area through guide tubes. Guide tubes are designed to minimize the amount of neutrons lost through the walls of the material. Quartz tubes are optimal, as it is nonmagnetic and allows for polarized neutron beams to be transported to the experiments. At UCN energies, the neutron wavelength is on the same order as visible light allowing for any properly coated "smooth" surface to be a good reflector. The guide tube is filled with ^{4}He gas at saturated vapour pressure. The probability of atomic interactions between the UCN and the He gas is extremely low and does not cause considerable loss in the neutron density [7]. Alternatively, we can place a thin window to isolate the ^{4}He from the experiments.

4 Monte Carlo N−Particle Modeling

4.1 Overview of MCNP

MCNP is a general-purpose **M**onte **C**arlo **N**−**P**article code that can be used for neutron, photon, electron transport. Neutron energies can vary from 10^{-11} MeV to 20 MeV for all isotopes. This places a cold neutron limit on the lowest energy neutrons that can be tallied (section 4.1.1). Monte Carlo simulations work by simulating individual particles as they pass through a user defined geometry. Aspects of the particles' average behaviour are then recorded. In MCNP these are known

as tallies.

In a Monte Carlo simulation, each event is calculated separate from the previous one, and large sample sizes are generally required to produce good statistical results. Each event involves simulating physical steps of particles through the geometry, making decisions about which physical processes might occur using a statistical sampling process that is dependent on random numbers. Each step is recorded throughout the particle's lifetime in the simulation. Each trial produces one neutron history. A large number of histories are required to generate an accurate picture of the neutron tracks and each track contributes to the user's preset tallies.

An alternative to the Monte Carlo method is the deterministic method, which breaks the geometry into infinitesimal boxes with the particles moving from one box to another, which can then be used to solve a neutron transport equation. Monte Carlo simulations can be used to duplicate a theoretically statistical process (such as neutron interactions) that can not be modeled in a straight forward manner through a deterministic method. Monte Carlo processes tend to mimic the statistical processes seen in actual particle physics experiments and are preferable to experimentalists for that reason.

4.1.1 Tallies in MCNP

Tallies can be constructed to track particle current, flux and energy deposition. Each cell or collection of cells defined by the input file could potentially hold one or more tallies. For example, if an input file defines a tally within a specific volume, say volume three, and asks that MCNP tally all neutrons that travel through this volume, the output file would contain the neutron flux passing through volume number three. The user can then modify this input file to ask only for neutrons at specific energies, and then MCNP will only count those neutrons that are within a specified neutron energy range, although the code will still complete the simulation for all energies passing through volume number three. The neutrons are not lost should they not fit the requirements to be tallied, since other tallies may require these neutrons. Heat deposition can also be measured, with MCNP providing the ability to differentiate between photon heating and neutron heating. Statistical error, R is calculated for each history, and for a well behaved tally, $R \propto \frac{1}{\sqrt{N}}$. In general an error of ≤ 0.10

is acceptable for each tally, although this error represents the statistical error of the calculation, not the accuracy compared to the actual physically observed value.

4.2 Neutron Sphere Moderation Test Model

4.2.1 Background

In Ref. [19], MCNP was used for neutron transport analysis to design and optimize the Low Energy Neutron Source (LENS) at Indiana University. The optimization included studies of materials and geometry used for the source.

The LENS cold neutron source uses proton-induced single neutron production to produce neutrons in the $1 - 10$ MeV range. A coupled moderator reduces these fast neutrons to cold energy levels. MCNP was used to provide accurate data for different moderating materials, at different thicknesses, for neutrons with an initial energy less than 10 MeV. Four different materials were selected for study as potential moderators, light water (H_2O), heavy water (D_2O), beryllium (Be), and graphite (C).

For one study in Ref. [19], an MCNP model geometry was designed to model an isotropic neutron source at the centre of a sphere, radius r, composed of these four different materials. The model was set to tally the thermal neutron flux within the sphere. The results for a sphere of $r = 40$ cm are displayed in Fig. 4, where the dashed lines indicate the work of Ref. [19].

This calculation was important for the design of LENS. It demonstrated that at energies between 3.5 Mev and 10 MeV, beryllium is a more effective neutron moderator than light water for producing thermal neutrons. In the end, light water was still used as a moderator for LENS, to minimize cost along with potential activation issues [19].

Also displayed in Fig. 4 is my own reproduction of this work using an MCNP simulation written from scratch. For my own work, this served as a highly relevant first exercise in order to learn how to use MCNP to produce results relevant to neutron moderation. I will now describe the process used to make this graph as an example of a typical MCNP simulation.

4.2.2 Input Files

Each data point on the graph in Fig. 4 represents one MCNP input file. To reduce the repetitive nature of creating multiple input files with the same geometry, but different moderating materials and initial neutron flux, a script in Perl was designed to create each input file, reading user input data for a set of six different parameters. These parameters included neutron source energy, the moderating material type, and its composition. The parameter values were inserted into a template with the different parameters input to create different MCNP trials. This allowed for simple modification of the geometry, source energy, along with the ability to increase the number of data points to acquire more precise data. MCNP was executed for each geometry simulation, ensuring that startup parameters were not identical for each trial, thereby ensuring the proper randomness that is expected for the simulation to produce accurate results. I used MCNP5 running on a Windows XP operating system for these trials.

4.2.3 Results

Output files containing the data of interest were automatically collected into a table for easy data analysis, using a custom Perl script. The data in this case was the total thermal neutron flux. My results are also shown in Fig. 4, along with the the reference results.

My data points generally follow the same trend as those from the reference. Error can be attributed mainly to two places. First, the volume of the tally was not discussed carefully in the reference, so as an assumption I chose a sphere of radius 5 cm, since this gave the most accurate results. Second, the exact definition of the neutron flux for the energy values given in Ref. [19] were not given. Through communication with the lead author on the paper (C. Lavelle), it was found that this crucial information had been lost. Given these two rather important uncertainties, the data points are surprisingly accurate accurate reconstruction of the graph. The general trends in the points are consistent, the normalization of the values on the vertical axis are reasonably close together.

The worst agreement in normalization is seen for carbon. Under further study, that normaliza-

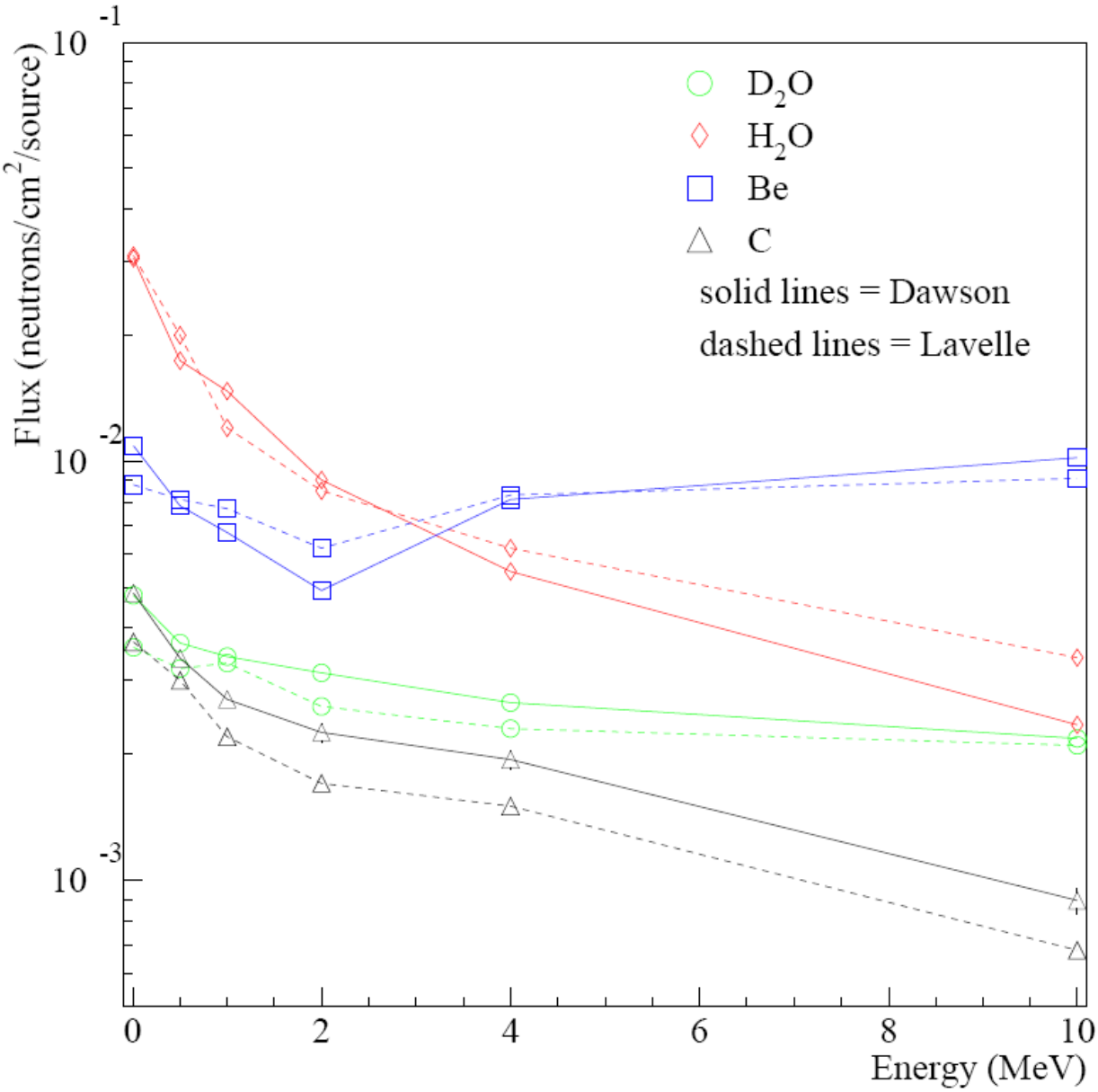

Figure 4: Simulated intensities of thermal neutron flux, for an isotropic neutron source of various energies ($T \leq 10$ MeV) at the centre of a sphere of radius $r = 40$ cm. Results shown are for four different moderating materials. Dashed lines show the reproduction of figure 5 from [19], using MCNP Monte Carlo simulation. Solid lines are this work.

tion was found to be strongly dependent on the carbon density used in the simulation. The density of graphite can vary broadly from sample to sample. It is therefore likely that Lavelle's work used a different density (lower) than my own.

4.3 Masuda Source Model

4.3.1 Background

In 2000, Y. Masuda proposed a spallation driven UCN source using a heavy metal target and UCN production in superfluid helium [20]. A similar technique can be attempted using reactor sources of neutrons. However, heat deposition in the superfluid by the numerous γ-rays produced in the reactor would make this method challenging since the superfluid must be maintained at $T < 1$ K.

To see if spallation would create enough cold neutron flux, along with manageable γ heating, he developed a UCN source geometry and modeled it in the LCS simulation code developed by a group at Los Alamos. The geometry is similar to the preferred geometry for TRIUMF. As a more challenging benchmark for our efforts to simulate cold neutron fluxes in UCN sources, we decided to attempt to reproduce the geometry in an MCNP simulation and its results.

Masuda's geometry is shown in Fig. 5.

4.3.2 Description in MCNP

MCNPX is the eXtended version on MCNP, allowing for protons to be modeled along with the particles present in MCNP. Proton modeling was necessary to accurately model the proton beam and proton induced spallation.

A source geometry was designed to be the same as the lower section of the UCN source shown in Fig. 5. The source consists of a lead spallation target situated in a D_2O bath at 300 K. The side of the target nearest the superfluid helium is gamma shielded with a small volume of Bismuth, to prevent gamma induced heating in both the 20 K moderator and the superfluid helium. Tallies are designed to find the total expected induced heating, due to both neutrons and photons, in both the superfluid He-II and the 20 K D_2O cold neutron moderator.

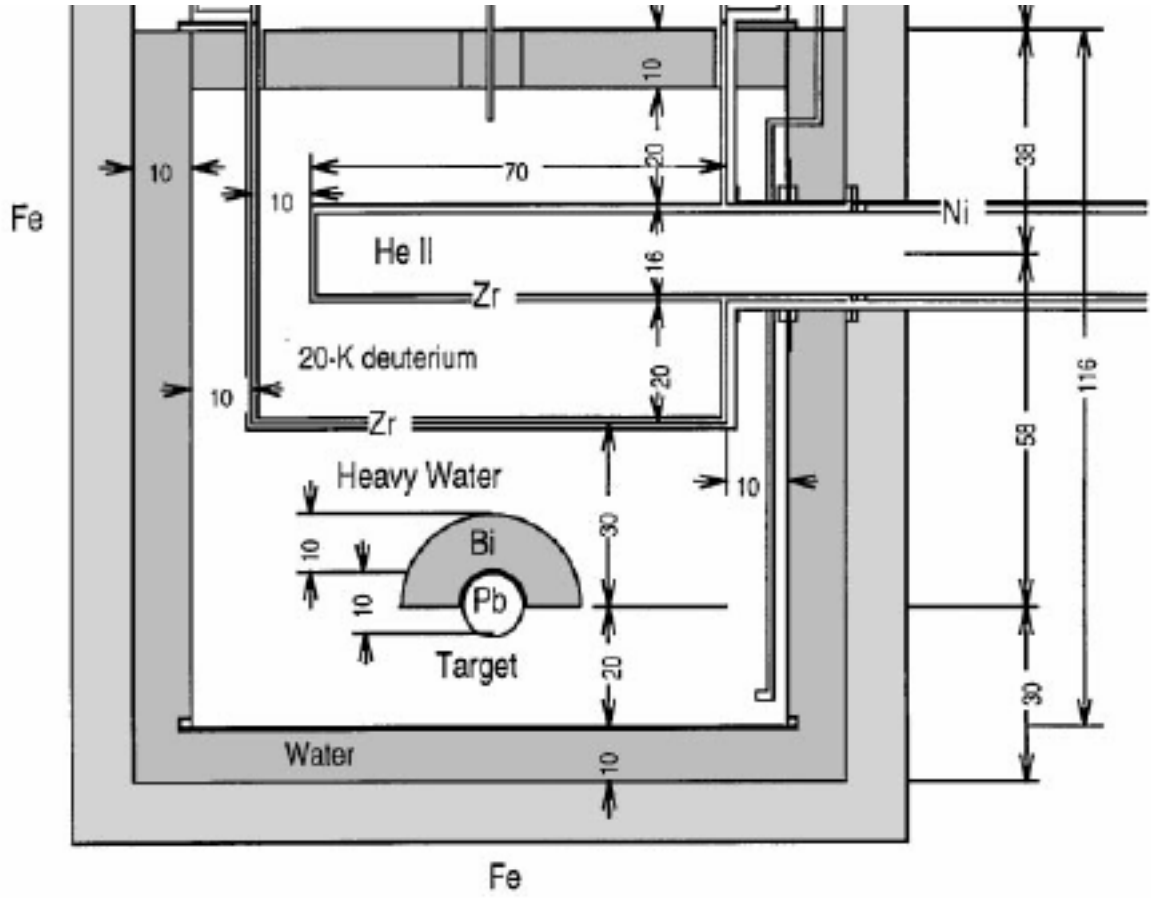

Figure 5: Early design of a spallation driven UCN source using downscattering in superfluid helium. Taken from Ref. [20].

Since MCNPX does not support simulations for calculating UCN densities by downscattering, cold neutron fluxes entering the superfluid helium are tabulated instead. The cold neutron flux can then be converted to an expected UCN density, as discussed in section 2.2.2. My reproduction of the geometry may be found in Fig. 6.

My results using the geometry shown in Fig. 6, are tabulated in Table 9.

Cold Neutron Flux	4×10^{11} n/cm^2/s
Heating in 20 K D_2O	15 Watts
Heating in He-II	0.5 Watts

Table 8: Results from Ref. [20]. For cold neutron flux and heating of the D_2O and He volumes.

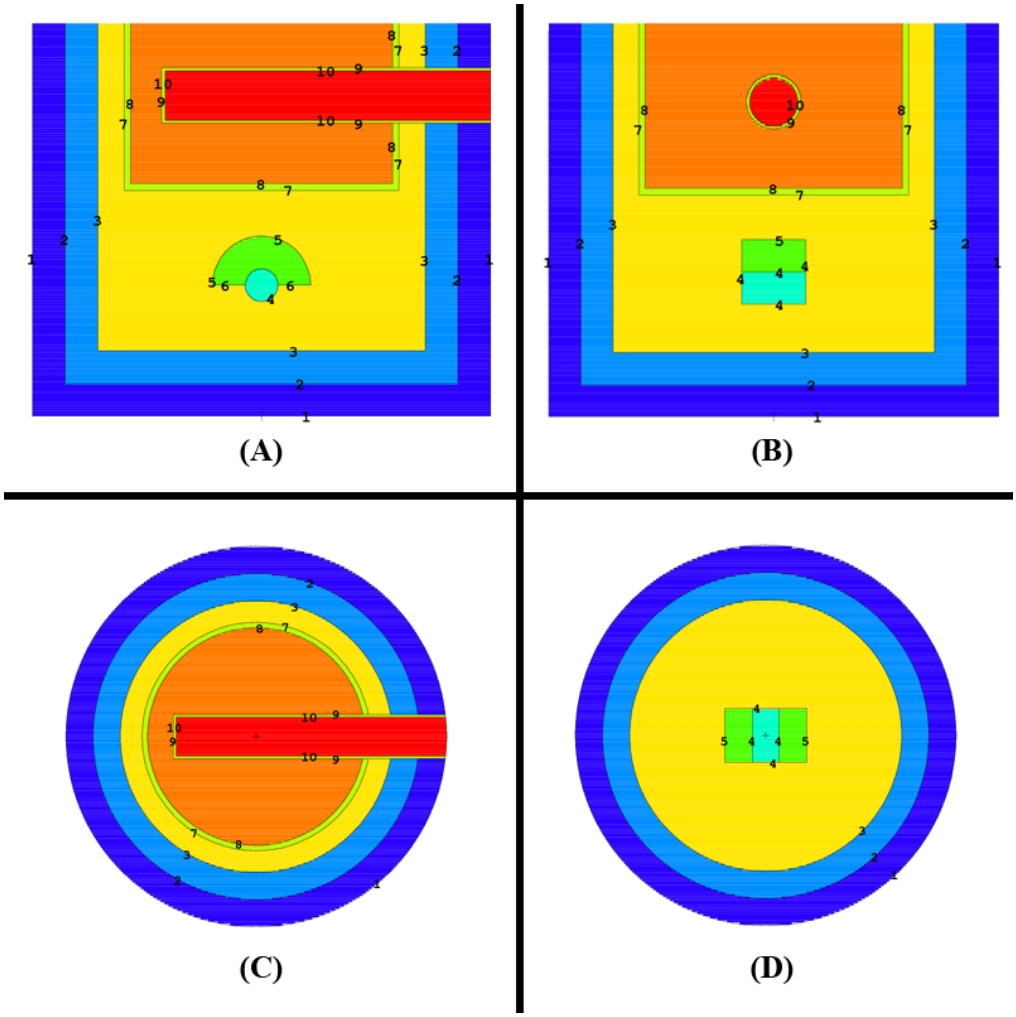

Figure 6: MCNPX reproduction of the source illustrated in Fig. 5. The numbers present on the diagram indicate where different cells end. Of interest are the superfluid helium [cell 10(red)] and the cold D_2 moderator [cell 8(orange)]. The spallation target is lead[cell 4(cyan)] surrounded by a 5 cm thick Bi γ-shield [cell 5 (green)]. Views at: (A)- XZ plane at $Y = 0$ cm. (B)- YZ plane at $X = 0$ cm. (C)- XY plane at $Z = 100$ cm. (D) XY plane at $Z = 41$ cm.

Cold Neutron Flux	1.15×10^{11} n/cm^2/s
Heating in 20 K D_2O	2.92 Watts
Heating in He-II	3.72×10^{-2} Watts

Table 9: Current Results

4.3.3 Results and Comparison with Masuda

The results listed in [20] are tabulated in table 8 and can be compared to my current results.

My results for each category are lower than the results listed in Ref. [20]. My results were 28.8%, 19.5% and 7.4% of the expected values for cold neutron flux, D_2O heating and He-II heating respectively. The most likely error was due in someway to geometry. Potentially there was some overall misunderstanding of the geometry presented in Fig. 5. Certainly, only the lower portion of the UCN source was modeled which could have contributed to some errors.

Perhaps most importantly the boundaries of the reference source were not clearly defined in the paper. Initially it was believed that cell 1 in Fig 5 was Fe, whereas on careful inspection of Ref. [20], it now appears it might be Pb, with a Fe volume surrounding the Pb. These aspects need to be taken into account for future considerations involving this geometry. This would lead to greater neutron reflection, resulting in more cold neutron flux, and also the increased heating, due mainly to enhanced γ-production.

As a reference source used to benchmark my MCNP model, my results are at least correct on an order-of-magnitude basis compared to Ref. [20]. This is encouraging given that it is known that small changes to geometry and material composition in a UCN source give rise to large changes in the cold neutron flux. It is for this reason that it is important to study these factors carefully and quantitatively. The deficiencies could not be addressed in this thesis due to lack of time.

4.4 Study of Optimization of Parameters

The heating of the superfluid He is a concern regarding the cold neutron flux. If the heat transport systems are unable to keep the helium cooled to 0.8 K, than upscattering will be increased and the UCN density will be reduced. One parameter of interest is the thickness of the Bi γ-shield (volume 5,6 in Fig. 10) and the relationship it has with the heat deposition in the superfluid helium. The

shield is present to absorb or scatter γ-rays and fast neutrons, while being relatively transparent to colder neutrons. The reduces the heat load in the superfluid. The thickness of this shield was varied in the MCNPX model to see its effect on cold neutron flux and the superfluid heat load.

4.4.1 Masuda *et al.* Discussion

In Ref. [21], a similar study was conducted for a Pb γ-shield along with the distance from the spallation source to the helium bottle.

The UCN source geometry used in that reference is shown is Fig. 7. In this figure, the thickness indicated by the number ② was varied. An increase in this thickness therefore consequently increases the target−to−helium distance.

Neutrons were produced in the target by a proton beam entering from either the left or the right. A lead shield directly adjacent to the target is there to reduce γ-induced heating of the rest of the source. The neutrons entered the two moderators to be cooled, eventually reaching the superfluid helium bottle. The produced UCN then traveled up out of the bottle into a UCN chamber.

Fig. 8 is a graphical representation of the results generated from varying thickness ②. As the thickness of the lead shield increased from 5 cm to 30 cm the amount of heat deposited in the helium was reduced by about 50%. The UCN production rate also reduced by about 50% over this same range. Based on this result, Masuda actually removed the γ-shield from the source to maximize the UCN production.

4.4.2 Discussion of My Results

In a similar fashion, I varied the Bi thickness in my model, keeping all other parameters constant, including the target−to−helium distance. An example of an altered geometry change is presented in Fig. 9 where Bi shield thickness has been increased to 20 cm. This can be compared to Fig. 10 with a thickness of 10 cm. Four different thicknesses of Bi were compared and the results are shown in Fig. 10.

My results show that the heat deposition dropped by about 25% as the Bi shield thickness increased from 5 cm to 20 cm. Cold neutron flux was plotted instead of UCN production rate as

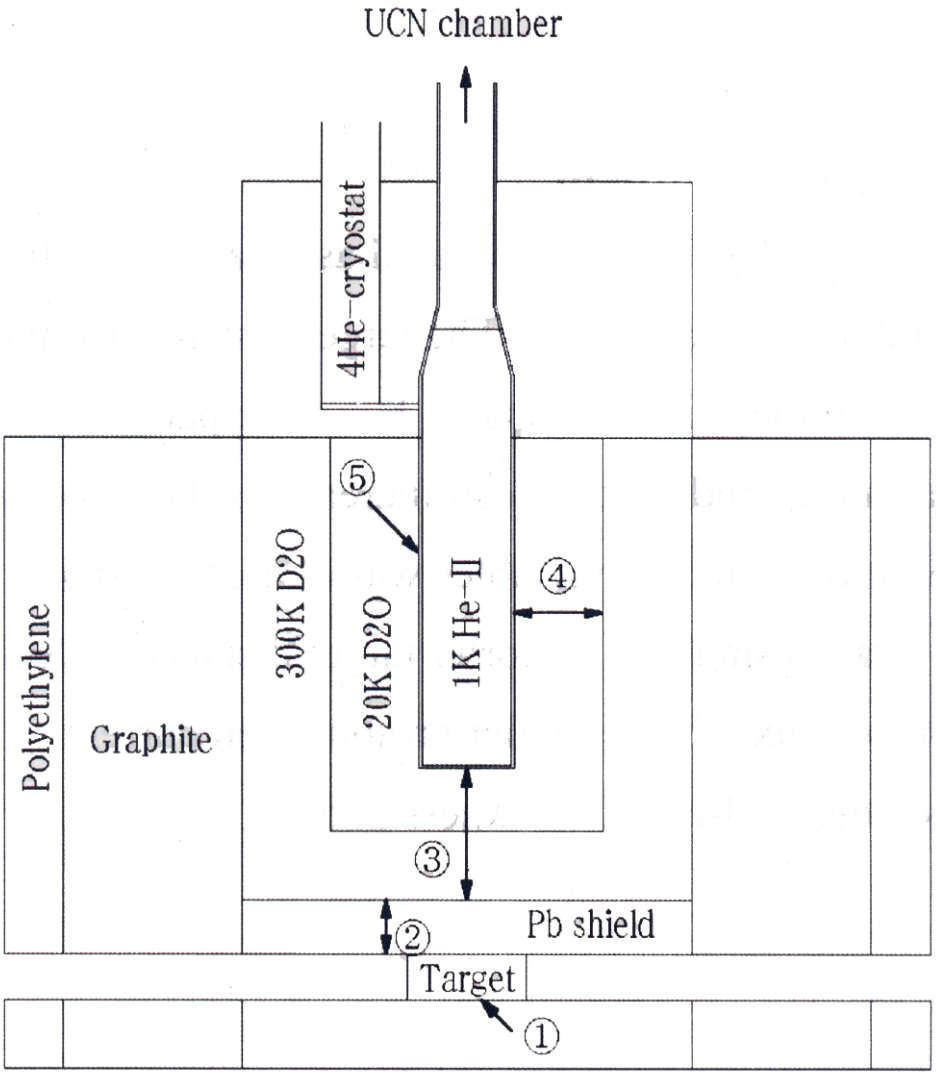

Figure 7: Basic configuration of UCN source. From Ref. [21]. (Side view) Features as discussed in the text

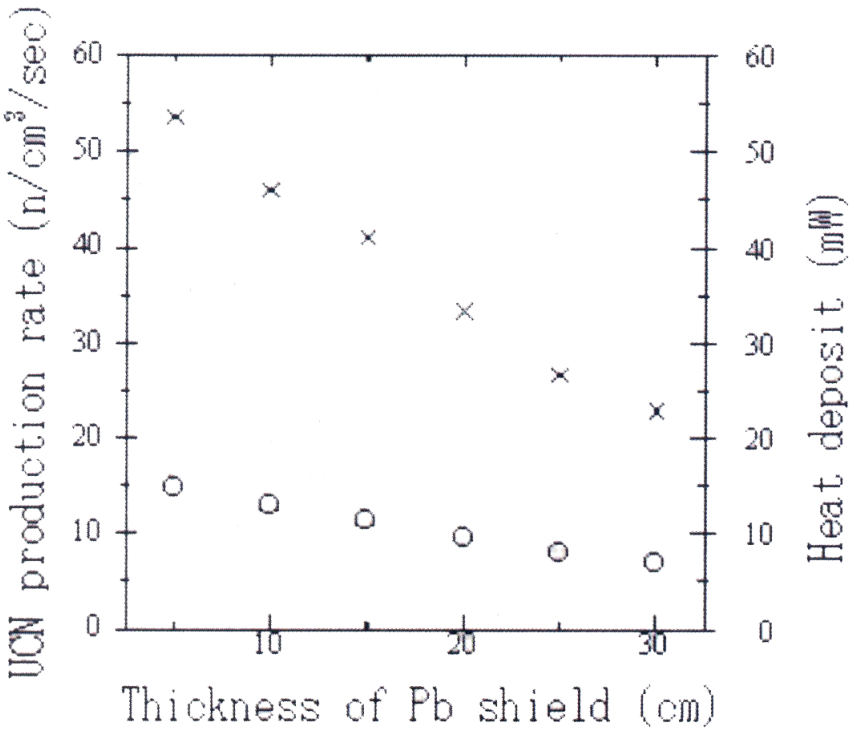

Figure 8: UCN production rate and heat deposition as functions of γ-shield thickness. Circles and crosses show the production rate of UCN and heat deposition, respectively. From Ref. [21].

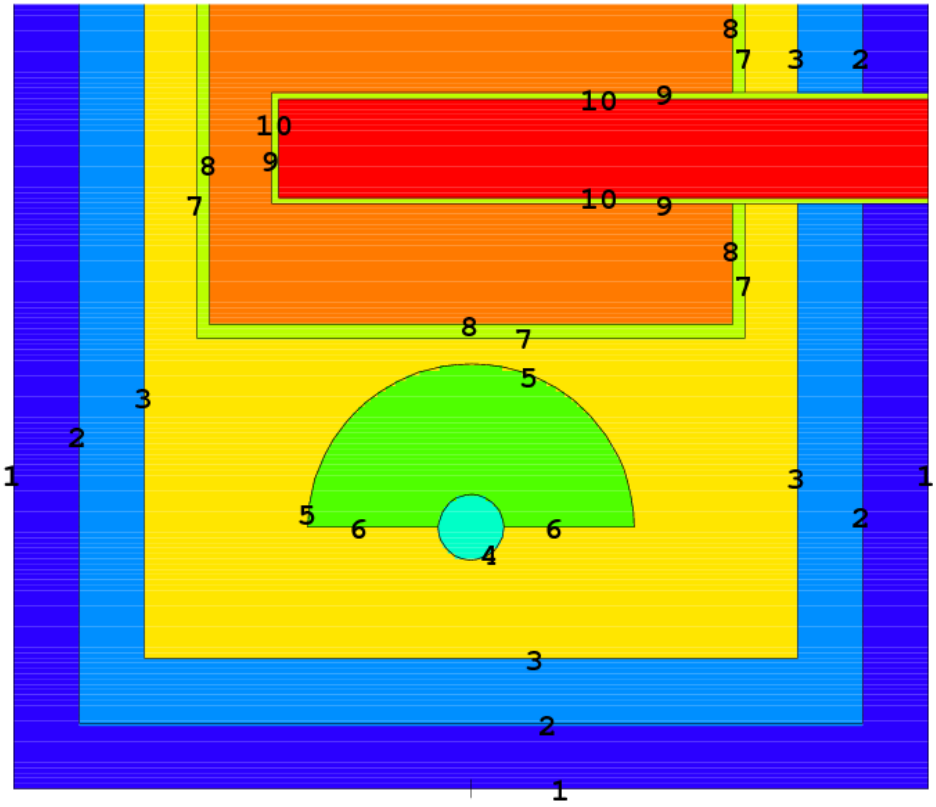

Figure 9: My geometry showing a variation of the Bi shield thickness, as compared to Fig. 6. The Bi shield is cell volume 5 (green) with a thickness of 15 cm.

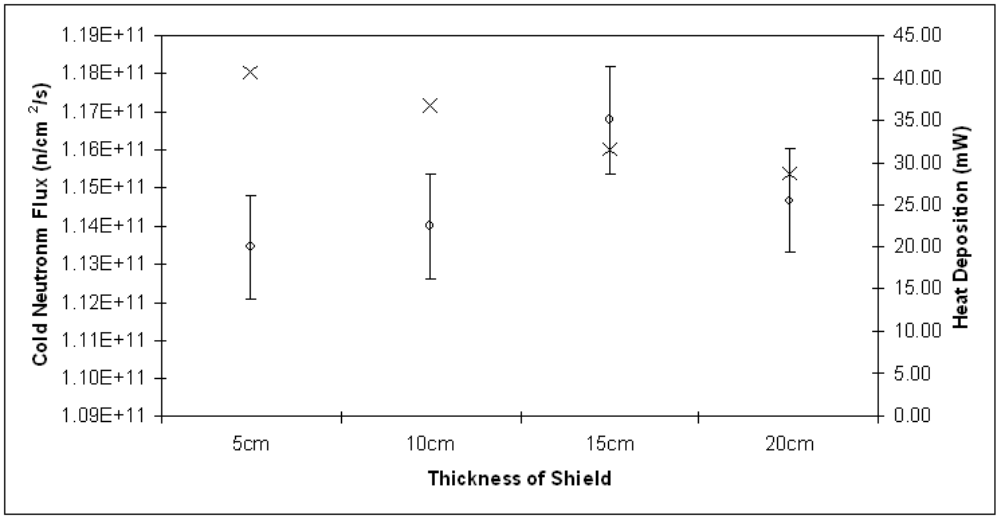

Figure 10: Using the source modeled in Fig. 6. Results shown for varying Bi shield thickness only. Circles and crosses show the cold neutron flux and heat deposition, respectively. Note the suppressed zero on the left hand vertical axis.

the conversion factor was not precisely calculated for this source. My results indicated that the cold neutron flux remained constant as the Bi shield thickness increased.

4.4.3 Comparison

Figure 10 appears to disagree Fig. 8. In Fig. 8 the production rate drops while in Fig. 10 the production remains constant. As discussed the geometry used for Fig. 8 varied the distance from the target along with varying the shielding thickness while my simulation did not. This difference in source geometries explains the increasing cold neutron flux obtained in this work.The increased difference likely causes the decreasing UCN production illustrated in Fig. 8 rather than the thickness of the shield.

5 Conclusion and Future Work

Ultracold neutrons are neutrons at extremely low energies, allowing for confinement in a material bottle by the Fermi pseudopotential of the walls. A high UCN density is desirable for next generation UCN experiments. The newly proposed CSUN source at TRIUMF aims to have the highest experimentally available UCN density. A first MCNP model of this new source was suc-

cessfully completed and cold neutron fluxes and heat loads were found to be in agreement on an order-of-magnitude basis with previous work. Furthermore, the simulation was used to study an important design parameter for the CSUN project: the thickness of a γ shield to reduce heat load in the superfluid UCN production volume. The results indicate that a heavy metal (Bi) shield can reduce γ-heating of the He while having little impact on the cold neutron flux or UCN density. This could be very important for CSUN because of the higher beam power at TRIUMF relative to the current UCN source in Japan. Ultimately we hope to modify this model to optimize the real source, ensuring maximal neutron production with manageable heating. Both concerns must be addressed in MCNP(X) before construction can begin on this new high density UCN source.

References

[1] R. Golub , D. Richardson and S. Lamoreaux, Ultra-Cold Neutrons. IOP Publishing Ltd, **1991**

[2] C. M. Lavelle, Ph.D Thesis, unpublished (2007)

[3] C. A. Baker *et al.*, Phys. Rev. Lett. **97**, 131801 (2006)

[4] J. W. Martin *et al.*, Canadian Ultracold Neutron Source, Proposal to TRIUMF. (May 27, 2008)

[5] V. Nesvizhevsky *et al.*, Nature **415**, 297 (2002)

[6] A. Serebrov *et al.*,Phys. Lett. B **72**, 605 (2005)

[7] Y. Masuda *et al.*, Phys. Rev. Lett. **89**, 284081 (2002)

[8] Y. Masuda, private communication.

[9] B. Hamermesh *et al.*, Phys. Rev. **90**, 603 (1953)

[10] E. T. Jurney *et al.*, Phys. Rev. C **25**, 2810 (1982)

[11] B. Filippone, private communication.

[12] S. Krane. Introductory Nuclear Physics. John Wiley & Sons Inc, **1988**

[13] Neutron scattering lengths and cross sections, http://www.ncnr.nist.gov/resources/n-lengths/

[14] P. Schmidt-Wellenburg *et al.*, Presented at the International Workshop on Particle Physics with Slow Neutrons, May 29-31, (2008) Grenoble, France. arXiv:0811.4332v2 [nucl-ex]

[15] K. van der Meer *et al.*, NIM Phys. Resc. B **217**, 202(2004)

[16] K. Tesch, Rad. Prot. Dosim. **11**, 165 (1985)

[17] http://www.bustertests.co.uk/studies/kinetics-collision-theory-maxwell-boltzmann-distribution.php

[18] M. Utsuro, Journal of Nuclear Science and Technology, **11**, 434 (1974)

[19] C. M. Lavelle *et al.*, NIM Phys. Resc. A **587**, 324 (2008)

[20] Y. Masuda *et al.*, NIM Phys. Resc. A **440**, 682 (2000)

[21] Y. Masuda *et al.*, Optimization of He-II UCN source with Spallation neutron source, Presented to the 15th Meeting of the International Collaboration on Advanced Neutron Sources (ICANS-XV) November 6-9, Tsukuba, Japan. (2000)